Climate Dynamics (2019) 53:943–956
https://doi.org/10.1007/s00382-019-04619-1

Sensitivity of ASCE-Penman–Monteith reference evapotranspiration under different climate types in Brazil

Daniela Jerszurki[1] · Jorge Luiz Moretti de Souza[2] · Lucas de Carvalho Ramos Silva[3]

Received: 23 August 2017 / Accepted: 8 January 2019 / Published online: 17 January 2019

Abstract
Sensitivity analysis of reference evapotranspiration (ETo) plays a key role in the simplification and improvement of measurements of terrestrial water balance. The aim of this study was to perform sensitivity analyses of the ASCE-Penman–Monteith reference ET equation (ETo_{PM}) for different tropical and subtropical climates, where a quantitative understanding of water fluxes to the atmosphere is limited. Sensitivity coefficients were derived on a daily basis for maximum and minimum air temperature, solar radiation, vapor pressure deficit and wind speed at 2 m height using data from 44-year of actual measurements for calibration (1970–2014), for nine different climatic zones across Brazil. A multiple regression analysis was performed to estimate the relation between meteorological data and ETo_{PM} across climatic zones. Seasonal and annual average estimates were obtained by averaging daily values and spatial patterns of ETo_{PM} were obtained by interpolating meteorological data from all sampled locations. Five climate variables were used in the analysis, which revealed diverse effects on ETo_{PM} across seasons and climatic zones. In order of importance, ETo_{PM} was most sensitive to annual variation in vapor pressure deficit (VPD), wind speed (U_2) and solar radiation (R_s) in all climate types. Our analysis also showed that VPD, calculated from measurements of relative humidity and temperature (T), are essential to accurately predict ETo_{PM} across tropical and subtropical climates. Due to the lack of direct meteorological measurements in many Brazilian regions, we recommend the adjustment of climate-driven hydrological fluxes predictions to the most sensitive variables, i.e., VPD, to improve the precision of reference ET losses. Our results will be useful in delineating the influence of different climatic variables in the ASCE Penman–Monteith model and in guiding new climatic modeling efforts in tropical and subtropical regions.

1 Introduction

Brazil is one of the most important producers of agricultural commodities in the world. Among other products, the country leads the world in production of coffee, sugar, ethanol and orange juice (MAPA—Brazilian Ministry of Agriculture, Livestock and Food Supply 2016), largely for exportation to Europe and the USA, with an expected increase of its international role in food production caused by increasing demand from Asian countries. To meet these demands the design of efficient irrigation systems is important to conserve water resources and achieve sustainable commercial crop production. In this context, reference evapotranspiration (ETo) is a critical parameter for designing irrigation systems, as well as for conducting climatological and hydrological studies. Rather than using the old term potential evapotranspiration, which is often ambiguously defined, we define ETo as the evaporation of water from soil and plant surfaces and transpiration from a reference crop defined as a hypothetical crop of 0.12 m height, surface resistance of 70 s m^{-1} and an albedo of 0.23. This might be considered the evaporation from an extensive surface of green grass of uniform height, actively growing and not short of water. The flux of water from the land to the atmosphere consists of plant transpiration, which strongly depends upon plant species and stage of development and, soil evaporation, which is affected by soil moisture and management practices (Allen et al. 1998). Thus, under well-watered conditions, the variability of climatic

✉ Daniela Jerszurki
dani_jerszurki@hotmail.com

[1] Wyler Department of Dryland Agriculture, French Associates Institute for Agriculture and Biotechnology of Drylands, Jacob Blaustein Institutes for Desert Research, Ben-Gurion University of the Negev, Sede Boqer, Israel

[2] Soil and Environment Studies Program, Federal University of Paraná, Curitiba, Paraná, Brazil

[3] Environmental Studies Program, Department of Geography, Institute of Ecology and Evolution, University of Oregon, Eugene, USA

variables, such as air temperature, relative humidity, solar radiation and wind speed, controls the flux of water from land to the atmosphere via plant transpiration and soil evaporation, which is directly related to the evaporative demand of the atmosphere. The ETo term is arguably the most important hydrologic variable currently used for estimation of agricultural water balances and recommended irrigation amounts in a wide variety of crops (Blaney and Criddle 1950; Xu and Singh 2005), and a key predictor of shifting biogeochemical cycles in natural ecosystems (Gatti et al. 2014). However, it is also the least understood of the biophysical processes currently being altered by climatic change (Silva 2015).

Over the past 50 years, empirical models have been developed to estimate ETo based on different combinations of climatic variables (Allen et al. 1998). The need to find accurate models to represent reference crops led to the Penman–Monteith equation (Monteith and Evaporation 1964), which is widely recognized as the standard method to estimate ETo. This method combines the first proposition (Monteith and Evaporation 1964) and adjustment (Allen et al. 1998) of Penman–Monteith method (Penman–Monteith FAO) and is now recognized as the standard approach to estimate ETo in different regions of the world, however, there is a growing need to improve ETo estimates in tropical and subtropical regions (Silva and Anand 2013). Recent isotopic studies have suggested that plant transpiration dominates the evapotranspiration fluxes (Jasechko et al. 2013), providing a quantitative path to the analysis of climate-induced changes in ET in agricultural and natural ecosystems, based on the analysis of plant tissues (Maxwell et al. 2014; Silva et al. 2015). Thus, following evidence that soil evaporation is negligible, simple and accurate estimates of reference ET may lead a better understanding of the dominant climate variables affecting transpiration flux. The reference ET estimates can be also easily adapted to assess plant evapotranspiration, through addition of plant and soil factors, such as water holding capacity, stomatal resistance to transpiration, and rooting characteristics (Jerszurki et al. 2017; Maxwell et al. 2018).

The Penman–Monteith equation is a physical–mathematical model derived from the energy balance and mass transfer of a system. In order to simplify the equation and enhance its applicability to different periodicities and reference surfaces (Walter et al. 2000; Itenfisu et al. 2003) the equation was updated (Penman–Monteith ASCE) by the American Society of Civil Engineers (ASCE) (Allen et al. 2005; Allen 2008). The new equation is similar to the Penman–Monteith FAO for daily periods, but with important differences in the way that the hourly fluxes are represented. The role of climate variables on the sensitivity of ETo is well described in the literature (Allen et al. 1998, 2005; Xu and Singh 2005; Monteith and Evaporation 1964; Saxton 1975; Rana and Katerji 1998; Hupet and Vanclooster 2001; Gong et al. 2006; Irmak et al. 2006; Chen et al. 2007; Liqiao et al. 2008; Estévez et al. 2009; Lemos Filho et al. 2010). However, there are few studies relating the sensitivity of the Penman–Monteith model under contrasting climatic conditions. For example, by analyzing the sensitivity of the Penman–Monteith model (Monteith 1965) in semi-arid regions, it was observed that calculations of ETo were highly sensitive to vapor pressure deficit (VPD) (Berengena et al. 2005) and solar radiation (R_s) (Rana and Katerji 1998). In contrast, a relatively greater influence of R_s and wind speed (U_2) was observed for wetter and colder regions (Hupet and Vanclooster 2001). In North America, the Penman–Monteith model outputs vary significantly depending on different combinations of VPD, U_2 and R_s that characterize different climatic zones (Irmak et al. 2006). Moreover, a strong dependency of the Penman–Monteith model to relative humidity (RH) was related in China, depending of the season and region (Gong et al. 2006; Liqiao et al. 2008).

In Brazil, the model has yet to be explored (Carvalho et al. 2011) and the Penman–Monteith FAO equation is commonly found in the Brazilian literature (Lemos Filho et al. 2010; Carvalho et al. 2011; Silva et al. 2011; Pereira et al. 2015, 2002; Souza et al. 2016), but the climatic data needed to validate the model are often not available, which limits its use. Even considering the different climate databases of meteorological data around world, as World Climate Database (Hijmans et al. 2005), a complete set of data needed to estimate ETo by the Penman–Monteith method is not available, because key variables such as wind speed, solar radiation, daily insolation and relative humidity are still missing. Testing the influence of different climate variables on the model by sensitivity analysis is therefore an important next step for developing simplifications and verifying the precision of ETo methods (Saxton 1975; Irmak et al. 2006). Accordingly, here for the first time in Brazil, we examine the sensitivity of ASCE Penman–Monteith ETo estimates to weather data for the most representative climate types. Our goal is to develop a better understanding of ETo variability to improve the standard Penman–Monteith model and possibly decrease the number of input variables needed for an accurate representation of different regions of the country.

2 Materials and methods

2.1 Climatic data

Analyses were carried out for a set of 26 National Meteorological Institute stations (INMET—Brazilian National Institute of Meteorology 2014) (Fig. 1) distributed across all Brazilian regions and most representative climate types (Álvares et al. 2013) (Table 1), with daily observations of maximum, minimum and average air temperature (°C), relative humidity (%), daily sunshine hours (MJ m^{-2} day^{-1}) and wind speed at 10 m height (m s^{-1}), from January 1970 to

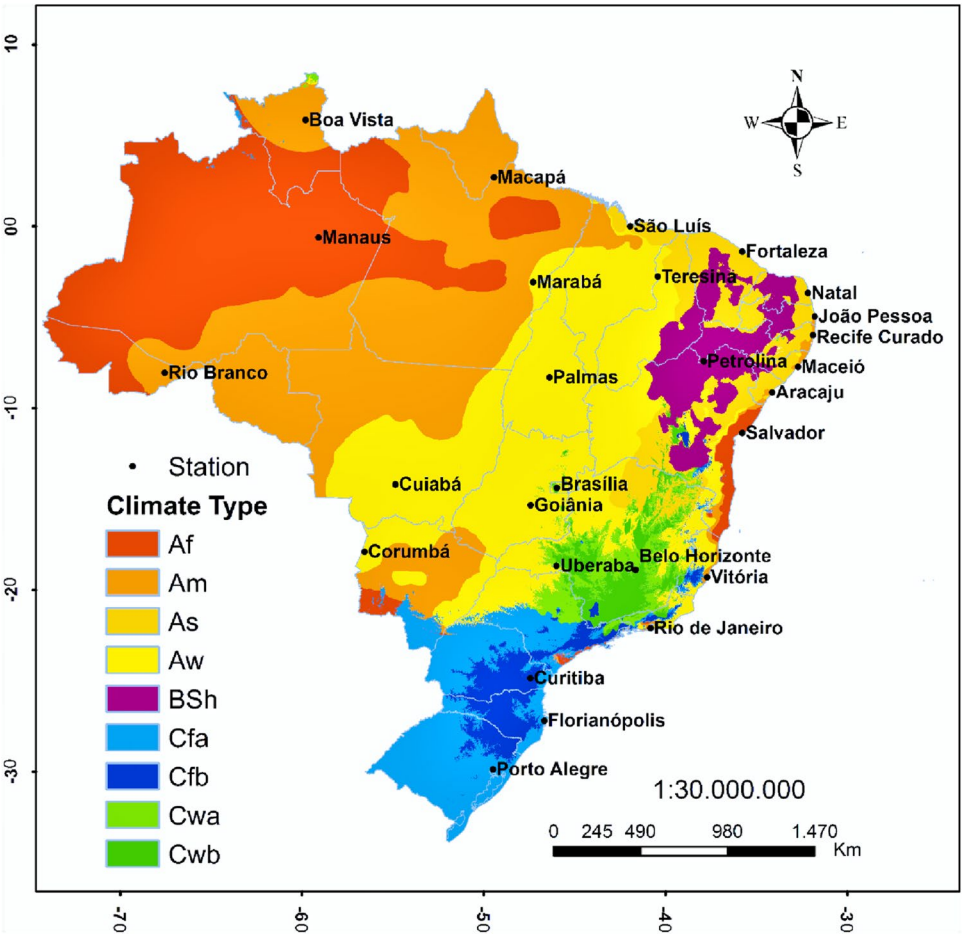

Fig. 1 Brazilian climatic zones and location of cities (meteorological stations) used in this study. Specific parameters for each climatic type are shown in Table 1

January 2014. The daily sunshine hours were measured by a heliograph Campbell-Stokes (model 240-1070-L). Daily wind speed was obtained at 10 m height by an anemometer Vaisala WT521 and transformed to wind speed at 2 m height by the wind profile relationship (Allen et al. 1998). Between 1970 and 2000, daily air temperature (maximum, minimum and average) and relative humidity were measured by one mercury thermometer and one capacitive sensor, respectively; and, between 2000 and 2014, the measurements were obtained by one Fluke 5699 thermometer and one humidity sensor Vaisala HMK15 respectively.

2.2 Penman–Monteith reference evapotranspiration (ETo_{PM})

Daily reference evapotranspiration was estimated by the Penman–Monteith method, parameterized by American Society of Civil Engineers (ASCE) (Allen et al. 2005).

$$ETO_{PM} = \frac{0.408 \cdot \Delta \cdot (R_n - G) + \gamma_{psy} \cdot \frac{C_n}{(T+273)} \cdot U_2 \cdot (e_s - e_a)}{\Delta + \gamma_{psy} \cdot (1 + C_d \cdot U_2)} \quad (1)$$

where ETo_{PM} is the reference evapotranspiration (mm day^{-1}); Δ is the slope of the saturated water-vapor-pressure curve (kPa °C^{-1}); R_n is the net radiation at the crop surface (MJ m^{-2} day^{-1}); G is the soil heat flux (MJ m^{-2} day^{-1}); γ_{psy} is the psychrometric constant (kPa °C^{-1}); T is the average daily air temperature (°C); U_2 is the wind speed at 2 m height (m s^{-1}); e_s is the saturation vapor pressure (kPa); e_a is the actual vapor pressure (kPa); C_n is the constant related to the reference type and calculation time step, considered equal to 900 for grass (dimensionless); and, C_d is the constant related to the reference type and calculation time step, considered equal to 0.34 for grass (dimensionless).

In the standardized Penman–Monteith method, the equations used to calculate aerodynamic and bulk surface resistance have been combined and reduced to two constants C_n and C_d (Allen et al. 2005). The constant C_n is a function of the aerodynamic resistance and time step and C_d is a function of the bulk surface resistance, aerodynamic resistance and time step, with the aerodynamic and bulk surface resistances varying according to the reference surface (Allen et al. 2000). Here we considered the constants C_n and C_d for a daily time step in a commonly used short reference crop (similar to grass) (Allen et al. 2000, 2005). Daily vapor

Table 1 Temperature and rainfall criteria for the complete Koppen's climate classification. Adapted from standard climatic classification (Álvares et al. 2013)

Symbol	Temperature (°C)			Rainfall (mm)			Climate
				Monthly		Annual	
	T_1	T_2	T_3	R_d	R_w		
Af	≥ 18			≥ 60		$\geq 25\ (100–R_d)$	Tropical without dry season
Am					< 60		Tropical monsoon
As						$< 25\ (100–R_{sdry})$	Tropical with dry summer
Aw						$< 25\ (100–R_{wdry})$	Tropical with dry winter
Bsh			≥ 18			$< 5.R_{LIM}$	Semi-arid with low latitude and altitude
Cfa	$-3 < T < 18$	≥ 22		> 40			Humid subtropical, oceanic climate without dry season, with hot summer
Cfb		$4 \leq T_{M10} < 22$					Humid subtropical, oceanic climate without dry season, with temperate summer
Cwa	$-3 < T < 18$	≥ 22		<40			Humid subtropical with dry winter and hot summer
Cwb		$4 \leq T_{M10} < 22$			$R_{swet} \geq 10.R_{wwet}$		Humid subtropical with dry winter and temperate summer

T_1 temperature of the coldest month; T_2 temperature of the hottest month; T_3 annual mean temperature; R_d rainfall of the driest month; R_w rainfall of the wettest month; R_{sdry} rainfall of the driest month in summer; R_{wdry} rainfall of the driest month in winter; R_{swet} rainfall of the wettest month in summer; R_{wwet} rainfall of the wettest month in winter; R_{LIM} rainfall of the driest month of the year; T_{M10} number of months where the temperature is above 10 °C

pressure deficit ($e_s - e_a$) was estimated by the difference between saturated and actual vapor pressure. Saturated vapor pressure was calculated using air temperature based on the Tetens formula (Murray 1967). Actual vapor pressure was obtained by saturated vapor pressure multiplied by relative humidity at each time step.

As the purpose of this work was to analyze the standard evapotranspiration method in Brazilian climate types, being useful as a guide for evapotranspiration studies, the radiation components were calculated according to the Penman–Monteith method (Allen et al. 1998), which is widely accepted and used in different climate conditions. Daily net radiation (R_n) is defined as the balance between net shortwave radiation (R_{ns}) and net longwave radiation (R_{nl}).

$$R_n = R_{ns} + R_{nl} \tag{2}$$

The R_{nl} is defined as the difference between outgoing and incoming longwave radiation, and as the outgoing longwave radiation is almost always greater than the incoming longwave radiation, R_{nl} represents an energy loss, being considered in this study as the "net outgoing" longwave radiation. On the other hand, the net shortwave radiation is normally positive and results from the balance between incoming and reflected solar radiation (R_s) (Allen et al. 1998). During daytime, net shortwave radiation flux is positive, net longwave radiation flux is negative and, thus, R_n was estimated by the difference between net shortwave radiation (R_{ns}) and net longwave radiation (R_{nl}).

The R_{nl} was obtained by air temperature, actual vapor pressure and relative shortwave radiation, which is the ratio of the solar radiation (R_s) to the clear-sky solar radiation (R_{so}).

$$R_{nl} = \sigma \cdot \left[\frac{(T_{max})^4 + (T_{min})^4}{2}\right] \cdot \left(0.34 - 0.14 \cdot \sqrt{e_a}\right) \cdot \left(1.35 \cdot \frac{R_s}{R_{so}} - 0.35\right) \tag{3}$$

where σ is the Stefan–Boltzmann constant (4.903×10^{-9} MJ K^{-4} m^{-2} day^{-1}); T_{max} is the maximum absolute temperature of the day (K); and, T_{min} is the minimum absolute temperature of the day (K).

The R_{so} represents the solar radiation that actually reaches the earth's surface in a given period under cloudless conditions. The following equation have been largely used in the tropics to estimate the R_{so} (Carvalho et al. 2013).

$$R_{so} = (0.75 + 2 \cdot 10^{-5} z) \cdot R_a \tag{4}$$

where z is the local altitude; and, R_a is the extraterrestrial radiation (MJ m^{-2} day^{-1}).

The R_{ns} is the fraction of the R_s that is not reflected from the surface, which is obtained as a function of the albedo (α).

$$R_{ns} = (1 - \alpha) \cdot R_s \tag{5}$$

The R_s was estimated by the relationship between extraterrestrial radiation (R_a) and relative sunshine duration (n/N), obtained from the ratio of the measured daily sunshine hours (n) to the maximum possible duration of sunshine or daylight hours (N), which expresses the cloudiness

of the atmosphere and accounts for differences in cloud cover across climatic zones.

$$R_s = R_a \cdot \left(a + b \cdot \frac{n}{N}\right) \quad (6)$$

where a is the linear coefficient; and, b is the angular coefficient.

The R_a was estimated as a function of the solar constant, latitude and the time of year (Allen et al. 1998).

$$R_a = \frac{24 \cdot (60)}{\pi} \cdot G_{sc} \cdot d_r \cdot [\omega_s \cdot sen(\phi) \cdot sen(\delta) + \cos(\phi) \cdot \cos(\delta) \cdot sen(\omega_s)] \quad (7)$$

where G_{sc} is the solar constant (MJ m^{-2} min^{-1}; G_{sc} = 0.0820 m^{-2} min^{-1}); d_r is the relative distance Earth–Sun (dimensionless); ω_s is the hourly angle corresponding to sunset (rad); φ is the latitude (rad); and, δ is the inclination of the sun (rad).

The soil heat flux (G) was calculated using air temperature (Wright and Jensen 1972).

$$G = 0.38 \cdot (T_d - T_{-3d}) \quad (8)$$

where T_{-3d} is the average daily air temperature of the previous 3 days.

Coefficients of variation (CV) were used to assess the variability of ETo_{PM} in response to weather data used in the ASCE Penman–Monteith model. Multiple regression analysis was used to correlate the estimated ETo_{PM} to climatic variables over climatic zones. Seasonal and annual average ETo_{PM} estimates were obtained by averaging daily values and the maps of spatial ETo_{PM} patterns were obtained by interpolating station values to all climatic zones in ArcGIS 10.1 (ESRI ArcGIS Desktop Release 10 2011).

2.3 Sensitivity analysis

In order to analyze the influence of each variable on ASCE Penman–Monteith, ETo were plotted relative to changes of a dependent variable against relative changes of the independent variables as a curve; i.e. a sensitivity coefficient curve (Goyal 2004). This simple mathematical approach has been widely used as a valuable and consistent way to characterize sensitivity (Saxton 1975; Rana and Katerji 1998; Hupet and Vanclooster 2001; Gong et al. 2006; Irmak et al. 2006). Due to the variability of dimensions and range values of climatic variables used in ASCE Penman–Monteith model, the use of a partial derivative as a non-dimensional form through daily sensitivity coefficients allows for its comparison (Smajstrla et al. 1987):

$$S_{vi} = \frac{\Delta ETo_{PMi}}{\Delta V_i} \quad (9)$$

where S_{vi} is the sensitivity coefficient for each i-day (dimensionless); ΔETo_{PMi} is the variation of ETo_{PM} by changes in the climatic variable for each i-day (mm day^{-1}); ΔV_i is the variation of the climatic variable for each i-day.

Were considered increasing and decreasing by 1 unit up to 5 units of daily T_{max}, T_{min}, VPD, R_s and U_2, over 44 years for all evaluated locations, while keeping other variables constant (Irmak et al. 2006). Considering the saturated vapor pressure (e_s) as an exponential function of air temperature (Allen et al. 1998), the increase/decrease of daily T_{max} and T_{min} was followed by changes of e_s and e_a and, then, of VPD in the sensitivity analysis. Due to significantly narrower ranges of VPD and U_2 compared to other variables, they were increased and decreased with 0.4 kPa and 0.5 m s^{-1} increments up to 2 kPa and 2.5 m s^{-1}, respectively.

The daily ETo_{PM} response to changes in each climatic variable was estimated by daily sensitivity coefficients. Each daily average sensitivity coefficient was estimated by the average of its increments for each climatic variable. The final daily average coefficient for each climatic variable was obtained by the averaging of 44 daily values, which corresponded to the 44 years of data. We used linear regression analysis to explain the linear relation between ΔETo_{PM} and ΔV for each climate type.

3 Results and discussion

3.1 Climatic conditions

Our observations showed large variability for all climatic parameters (T_{max}, T_{min}, RH, R_s, U_2 and VPD) across Brazilian regions, spanning humid subtropical (Cfa, Cfb, Cwa and Cwb), tropical with dry summers (As), and semi-arid (Bsh) regions throughout the year (Table 2). This large variability indicates the existence of different sensitivity coefficients for predicting ETo throughout the country. In general, VPD was the most variable in humid climatic zones. High T_{max} and T_{min} and low RH in semi-arid climate (Bsh) resulted in the highest VPD across all climatic zones.

The coefficients obtained by multiple regression analysis (Table 3) show the largest effect of VPD on ETo estimations over climate types and seasons, suggesting that the major changes in ETo are the result of the dynamic of atmospheric water demand over time. Indeed, the importance of VPD on ETo has been related at different climate zones around the world (Rana and Katerji 1998; Irmak et al. 2006; Lemos Filho et al. 2010; Silva et al. 2011). According to the first estimates of water evaporation, originally done by Dalton (Shaw 1993), evaporation was considered a main result of the vapor pressure deficit, which represents the atmospheric demand in the Penman–Monteith equation (Allen

Table 2 Annual daily average and coefficient of variation of the climatic variables over the study period and climate type

Climate	Variable	Annual Average	CV (%)				
			Annual	Summer	Autumn	Winter	Spring
Af	T_{min} (°C)	22.74	2.64	1.34	1.54	1.61	1.50
	T_{max} (°C)	29.83	2.42	1.33	1.75	1.97	1.45
	RH (%)	73.77	3.14	1.89	1.88	2.52	2.05
	VPD (kPa)	0.66	13.00	4.71	6.59	10.80	7.40
	R_s (MJ m^{-2} day^{-1})	18.06	9.54	3.17	7.53	8.51	3.47
	U_2 (m s^{-1})	1.73	8.45	6.00	6.11	7.00	6.79
	ETo_{PM} (mm day^{-1})	3.73	11.10	3.37	8.67	9.97	3.22
Am	T_{min} (°C)	22.22	4.03	0.48	2.94	1.71	1.63
	T_{max} (°C)	30.37	2.31	0.49	2.06	1.31	0.80
	RH (%)	79.02	2.30	0.49	0.98	2.09	1.05
	VPD (kPa)	0.76	10.96	2.34	8.02	9.93	2.81
	R_s (MJ m^{-2} day^{-1})	18.56	10.13	2.53	6.97	8.05	2.08
	U_2 (m s^{-1})	1.98	13.84	3.89	7.19	11.90	2.86
	ETo_{PM} (mm day^{-1})	3.97	15.71	14.24	9.84	10.74	2.27
As	T_{min} (°C)	23.41	4.52	0.87	2.26	1.83	2.03
	T_{max} (°C)	30.01	2.14	0.33	1.44	0.93	0.86
	RH (%)	78.41	3.95	1.71	1.07	3.02	0.85
	VPD (kPa)	0.78	16.46	6.67	7.21	11.90	2.57
	R_s (MJ m^{-2} day^{-1})	21.04	11.49	3.76	5.55	10.29	2.32
	U_2 (m s^{-1})	3.14	14.53	8.26	7.07	8.90	5.50
	ETo_{PM} (mm day^{-1})	4.45	14.12	4.46	6.85	12.33	2.40
Aw	T_{min} (°C)	20.68	7.42	0.52	5.76	6.13	1.27
	T_{max} (°C)	31.45	3.23	0.70	1.22	3.66	2.06
	RH (%)	71.74	11.27	1.67	4.76	6.84	6.80
	VPD (kPa)	0.98	31.28	8.09	12.58	16.88	17.82
	R_s (MJ m^{-2} day^{-1})	18.98	6.87	3.02	3.09	6.23	3.38
	U_2 (m s^{-1})	1.47	12.39	6.61	7.39	8.57	5.45
	ETo_{PM} (mm day^{-1})	4.09	12.83	4.17	4.02	12.49	5.68
Bsh	T_{min} (°C)	22.01	5.86	0.97	3.74	2.32	2.63
	T_{max} (°C)	32.14	4.66	1.22	2.50	3.58	1.29
	RH (%)	55.37	10.49	5.20	2.73	8.18	6.55
	VPD (kPa)	1.59	18.44	11.93	6.26	15.94	4.78
	R_s (MJ m^{-2} day^{-1})	17.71	11.98	4.13	8.55	10.75	3.19
	U_2 (m s^{-1})	2.28	12.34	8.36	10.05	6.23	6.82
	ETo_{PM} (mm day^{-1})	4.28	16.12	8.21	7.50	15.00	3.51
Cfa	T_{min} (°C)	16.44	20.84	2.11	15.70	8.00	9.06
	T_{max} (°C)	24.93	13.94	1.88	10.23	4.32	7.57
	RH (%)	78.51	3.50	2.16	2.40	2.26	2.51
	VPD (kPa)	0.57	30.30	7.98	22.72	13.88	17.42
	R_s (MJ m^{-2} day^{-1})	17.01	26.51	8.14	17.88	18.17	9.80
	U_2 (m s^{-1})	2.57	19.84	9.01	14.01	16.28	6.30
	ETo_{PM} (mm day^{-1})	3.14	37.78	8.91	27.66	26.88	14.01
Cfb	T_{min} (°C)	13.08	2.57	2.57	2.57	2.57	2.57
	T_{max} (°C)	23.43	23.53	2.57	19.05	10.74	9.92
	RH (%)	81.22	11.33	2.03	8.88	5.09	7.14
	VPD (kPa)	0.44	2.46	1.35	1.26	2.91	2.27
	R_s (MJ m^{-2} day^{-1})	16.31	19.44	7.23	14.55	16.53	15.99
	U_2 (m s^{-1})	2.10	20.53	6.66	14.17	13.60	8.99
	ETo_{PM} (mm day^{-1})	2.78	12.64	7.50	8.56	9.49	6.36

Table 2 (continued)

Climate	Variable	Annual Average	CV (%)				
			Annual	Summer	Autumn	Winter	Spring
Cwa	T_{min} (°C)	17.12	16.96	4.00	15.24	14.32	5.75
	T_{max} (°C)	29.95	6.28	4.08	5.74	7.66	4.73
	RH (%)	65.88	15.21	4.37	7.30	13.39	11.79
	VPD (kPa)	1.06	30.15	14.98	12.74	23.38	26.75
	R_s (MJ m^{-2} day^{-1})	18.69	13.04	9.63	11.14	11.36	11.71
	U_2 (m s^{-1})	1.11	41.10	31.42	36.95	31.37	33.95
	ETo_{PM} (mm day^{-1})	3.86	19.91	12.06	15.92	20.90	13.09
Cwb	T_{min} (°C)	17.38	11.30	1.44	10.14	6.86	3.35
	T_{max} (°C)	27.21	5.20	1.98	4.79	4.30	1.96
	RH (%)	68.10	7.52	3.31	2.96	4.98	6.60
	VPD (kPa)	0.92	13.67	10.09	5.78	13.62	14.77
	R_s (MJ m^{-2} day^{-1})	18.52	12.58	5.78	9.38	9.65	5.34
	U_2 (m s^{-1})	1.50	10.37	9.04	6.41	11.05	8.96
	ETo_{PM} (mm day^{-1})	3.61	18.81	5.94	15.10	17.60	5.23

et al. 1998). These results also show the importance of VPD as an essential variable to accurately predicting ETo in the standard method as well as an important next step to the development of new simplified ET methods. The alternative methods are useful when the complete set of data needed to solve the Penman–Monteith method is incomplete or not available, which is often the case in Brazil.

We observed high and constant ETo_{PM} throughout the year in the semi-arid climate (Bsh). Despite relatively small VPD, the range of ETo_{PM} in tropical climates (Af, Am, As and Aw) was similar to semi-arid regions (Bsh) (Fig. 2), mainly due to the great R_s observed in tropical climates (Álvares et al. 2013). Under tropical conditions, mainly in winter periods, the high R_s offset the small VPD to maintain the ETo_{PM}, which has been related to the maintenance of high plant productivity. The link between solar radiation, ETo_{PM} and the ecosystem primary production is not well-know and its response is highly variable, which can strongly depend upon the seasonality and cyclicality of weather events (Clark et al. 2003; Fearnside 2004). However, our results are in line with those obtained for tropical regions over wet seasons, when decreases in cloud cover may cause an increase in ETo_{PM} (Butt et al. 2009). Despite the main goal of this work being to analyze the standard ET method itself and even the main procedures for estimating solar radiation described in the Penman–Monteith equation have been largely used in the tropics, we highlight the importance of the development and use of different solar radiation methods. These methods should take into account the effect of weather conditions, such as cloud cover and high relative humidity, being useful for different climatic zones (Yan et al. 2012). We observed the lowest ETo_{PM} under subtropical climates (Cfa, Cfb, Cwa and Cwb), but with high variability over seasons (Fig. 2). The annual results indicated a clear separation between tropical (Af, Am, As and Aw), semi-arid (Bsh) and subtropical (Cfa, Cfb, Cwa and Cwb) climate types (Fig. 2). In summer, autumn and spring, we observed marked differences between warm (Af, Am, As, Aw and Bsh) and cold (Cfa, Cfb, Cwa and Cwb) climate types. Regional and seasonal effects are important, as shown by the amplitude of the ETo variation across regions (25.2%) and seasons within (2.2% in spring to 28% in summer) and across all climatic zones combined (24.8%). In contrast with the tropical (Af, Am, As and Aw) and semi-arid (Bsh) climates, T_{max} and T_{min} showed high variability over the year in humid subtropical climates (Cfa, Cfb, Cwa and Cwb), due to its strong seasonality, mainly in the autumn and winter seasons (Table 2). In addition, R_s was highly variable, mainly under wet and cold conditions but with low seasonality (0.35% in winter to 0.78% in spring) within regions.

3.2 Sensitivity coefficients

The variation of ETo_{PM} as a function of changes in each climatic variable represented annual average values and did not shown the seasonal variability of sensitivity (Fig. 3). The sensitivity coefficients are presented in the Fig. 4. The information provided by the sensitivity coefficients is essential to quantify uncertainties of ETo_{PM} estimates.

As observed in some Brazilian regions and around the world (Irmak et al. 2006; Liqiao et al. 2008; Lemos Filho et al. 2010), our results show a strong and linear response of ETo_{PM} to changes in climatic variables ($R^2 \geq 0.98$) for all climate types (Fig. 3). The T_{max} and T_{min} showed low influence on ETo_{PM} on annual basis (Fig. 4a, b). Considering the saturated vapor pressure (e_s) as an exponential function of air temperature and ETo_{PM} as a linear function of VPD, the increasing temperature results in increasing ETo_{PM} (Allen et al. 1998). Indeed, in this study, increasing

Table 3 Model summaries of multiple regressions for prediction of daily and seasonal ETo_{PM} over climate types

Variable	Climate	Coefficient (b)					Climate	Coefficient (b)					Climate	Coefficient (b)				
		Annual	Summer	Autumn	Winter	Spring		Annual	Summer	Autumn	Winter	Spring		Annual	Summer	Autumn	Winter	Spring
T_{min} (°C)	Af	0.08	0.00	0.05	0.04	0.08	Aw	0.08	0.06	0.05	0.06	−0.10	Cfb	0.07	0.07	0.07	0.07	0.13
T_{max} (°C)		0.00	0.02	−0.03	−0.02	−0.04		−0.13	−0.10	−0.08	−0.12	−0.09		−0.04	−0.07	0.00	−0.04	−0.03
RH (%)		−0.02	−0.01	0.00	0.00	0.00		0.11	0.10	0.11	0.10	0.10		0.03	0.04	0.00	0.02	−0.02
VPD (kPa)		0.15	0.76	0.74	0.49	0.68		3.85	3.56	3.48	3.38	3.46		2.43	2.44	1.31	2.44	0.80
R_s (MJ m^{-2} day^{-1})		0.21	0.17	0.22	0.21	0.14		0.16	0.15	0.17	0.18	0.16		0.15	0.17	0.13	0.14	0.13
U_2 (m s^{-1})		0.09	0.02	0.04	0.24	0.08		0.10	0.11	−0.10	0.14	0.18		0.22	0.18	0.11	0.25	0.19
Constant		−1.22	0.25	−1.27	−1.25	0.05		−8.88	−8.25	−9.06	−7.73	−4.08		−3.49	−3.50	−1.49	−2.99	0.85
R^2		0.98	0.84	0.97	0.98	0.85		0.99	0.96	0.92	0.98	0.94		0.99	0.95	0.99	0.97	0.98
F		2.830*	73.700*	485.500*	744.640*	79.340*		4.410*	348.840*	161.260*	854.710*	213.440*		8.490*	289.600*	1.040*	523.580*	764.380*
Error variance		–	–	–	–	–		–	0.01	0.01	0.01	0.01		–	–	–	0.01	–
T_{min} (°C)	Am	0.00	0.24	0.10	0.04	0.14	Bsh	0.08	−0.01	0.13	0.05	0.03	Cwa	0.11	0.02	0.08	0.02	−0.01
T_{max} (°C)		−0.12	−0.03	−0.07	0.01	0.00		0.03	−0.11	−0.02	0.05	0.20		−0.05	−0.05	−0.04	−0.04	0.01
RH (%)		0.22	−0.04	0.08	0.04	−0.02		−0.01	−0.04	−0.01	−0.02	0.01		0.00	0.02	0.01	0.02	−0.01
VPD (kPa)		4.92	0.02	2.26	1.69	0.71		0.69	0.51	0.29	1.31	0.40		0.73	1.47	0.47	1.63	0.45
R_s (MJ m^{-2} day^{-1})		0.21	0.16	0.19	0.16	0.14		0.17	0.10	0.16	0.07	0.07		0.18	0.18	0.18	0.14	0.12
U_2 (m s^{-1})		0.54	0.29	0.31	0.40	0.21		0.58	0.90	0.35	0.78	0.63		0.27	0.14	0.21	0.40	0.15
Constant		−18.59	−0.89	−8.61	−5.06	−1.30		−3.62	6.49	−1.83	−2.80	−6.49		−0.94	−1.37	−1.27	−1.85	1.74
R^2		0.75	0.82	0.99	0.99	0.88		0.97	0.92	0.90	0.96	0.65		0.86	0.62	0.86	0.91	0.69
F		184..45*	63.680*	1.310*	1.740*	106.510*		1.770*	162.040*	129.730*	383.460*	26.160*		368.140*	22.860*	87.960*	150.390*	31.450*
Error variance		0.10	–	–	–	–		–	0.01	0.01	0.01	0.01		0.08	0.10	0.04	0.06	0.11

Table 3 (continued)

Variable	Climate	Coefficient (b)					Climate	Coefficient (b)					Climate	Coefficient (b)				
		Annual	Summer	Autumn	Winter	Spring		Annual	Summer	Autumn	Winter	Spring		Annual	Summer	Autumn	Winter	Spring
T_{min} (°C)	As	0.05	0.00	0.21	0.08	0.04	Cfa	0.10	0.17	0.07	0.11	0.11	Cwb	0.08	0.02	0.10	0.09	0.04
T_{max} (°C)		0.04	0.07	−0.03	−0.03	0.09		−0.11	−0.12	−0.08	−0.08	−0.09		−0.10	−0.11	−0.04	0.01	−0.04
RH (%)		0.00	0.05	−0.02	0.00	−0.04		0.04	0.00	0.03	0.02	0.03		0.06	0.09	0.03	0.02	0.04
VPD (kPa)		1.21	2.12	0.64	1.48	1.03		3.08	1.62	3.04	1.85	2.83		2.28	3.07	1.17	0.85	1.49
R_s (MJ m^{-2} day^{-1})		0.17	0.15	0.13	0.15	0.14		0.17	0.18	0.15	0.16	0.15		0.20	0.17	0.17	0.18	0.17
U_2 (m s^{-1})		0.03	0.12	0.01	0.16	0.09		0.10	0.11	0.12	0.10	0.06		0.49	0.35	0.30	0.63	0.34
Constant		−2.13	−6.75	−1.72	−1.05	−0.44		−3.87	−0.90	−2.82	−2.07	−3.01		−5.35	−6.52	−3.93	−4.42	−3.60
R^2		0.99	0.92	0.96	0.99	0.94		0.99	0.98	0.99	0.98	0.99		0.98	0.97	0.99	0.99	0.94
F		8.430*	160.690*	380.140*	3.240*	234.230*		2.250*	670.660*	3.150*	896.690*	1.380*		5.300*	512.610*	1.890*	1.770*	222.510*
Error variance		–	−F	–	–	–		–	–	–	–	–		0.08	–	0.05	0.04	0.08

*Significant at the $P = 0.05$ level

air temperature, while keeping other variables constant, resulted in a slight increase in ETo_{PM} (Fig. 3). The increment of air temperature tends to increase the atmospheric evaporative demand through increase in VPD (Murray 1967; Sulman et al. 2016). In general, a 1 °C increase in maximum and minimum air temperature resulted in 0.06 mm day^{-1} and 0.03 mm day^{-1} increase in ETo_{PM}, respectively (Fig. 3). When the VPD is kept constant, the influence of air temperature on ETo_{PM} declines (Irmak et al. 2006; Silva et al. 2011). In combination with our results, this finding suggests that air temperature is the weakest factor directly influencing ETo_{PM}. However, for arid climates (Bsh), with rainfall around 100–400 mm $year^{-1}$ and RH around 40% in the winter period, even a small increase in temperature results in a significant increase in ETo_{PM}. In this climate zone, ETo_{PM} varied between ± 14% in response to the change in temperature by ± 20% (Goyal 2004).

Under tropical (Af, Am, As and Aw) climates we observed low influence of air temperature on ETo sensitivity (Fig. 4a, b), as already observed in previous studies for Northern Brazil (Fisch et al. 1998). However, contrasting to the results observed in warm and humid climates in other regions of the world (Irmak et al. 2006). In coastal areas of California and Florida, for example, the maximum temperature is high and is generally associated with high RH, which reaches up to 97% in the winter period, resulting in a low vapor pressure deficit (Irmak et al. 2006). Thus, shifts in temperature have a greater influence in Penman–Monteith model, due to the small influence of VPD and R_s, when compared to Brazilian tropical climates. This finding has far-reaching consequences for predicting temperature-induced changes in the regional hydrological and biogeochemical cycle (Gatti et al. 2014).

Estimated VPD showed the largest sensitivity coefficients, being strongly correlated with ETo_{PM} in all climate zones (Figs. 3, 4c). However, the sensitivity gradually decreased toward summer owing to changes in maximum temperature (Fig. 4c). Increasing air temperature decreases the magnitude of the slope of the saturation vapor pressure curve in the Penman–Monteith model (Irmak et al. 2006; Monteith and Unsworth 1990). Based on this same principle, we observed larger sensitivity to VPD in cold climates (Cfa, Cfb, Cwa and Cwb) over the year (Fig. 4c). The semiarid climate (Bsh) showed the largest sensitivity among climates, especially during winter months (Fig. 4c). In semiarid regions, low relative humidity favored larger VPD's, which increased the sensitivity of ETo_{PM}, especially during winter when the influence of air temperature is lower (Fig. 4a, b). A 0.4 kPa increase in VPD resulted in a 1.64 mm day^{-1} increase in ETo_{PM} in semiarid climate, reaching 2 mm day^{-1} during winter months (Fig. 4c). Consistent with our results, the influence of saturated vapor pressure on atmospheric water demand has been observed in semiarid regions (Wang

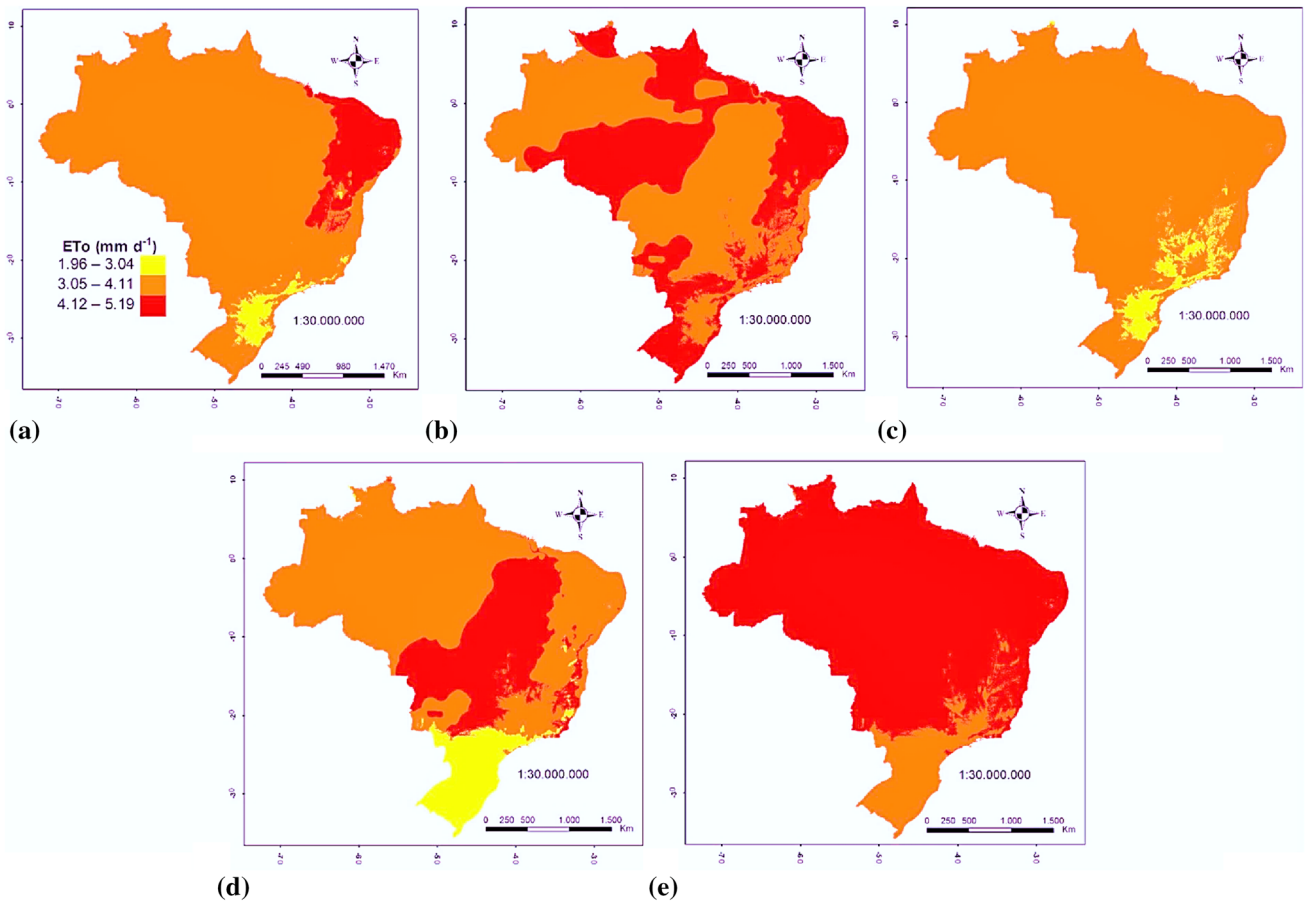

Fig. 2 Spatial distribution of average daily ETo_{PM} during the study period for all climate types to the annual (**a**), summer (**b**), autumn (**c**), winter (**d**) and spring (**e**) periods

and Dickinson 2012) under conditions like those found in Northeastern Brazil.

The sensitivity to VPD in subtropical climates can also be explained by the lower R_s occurred in these regions compared to the tropical regions (Table 2). Thus, there is a reduction of the term corresponding to the radiation component in the Penman–Monteith model rather than the variables related to the atmospheric demand. The influence of VPD about ETo_{PM} is even larger due to its range interval (Table 2), with small variations in VPD resulting in large variations of ETo_{PM}.

Solar radiation had a diverse effect on ETo_{PM} in different climates (Fig. 3), being higher and more constant over year in warm and humid climates (Af, Am, As and Aw) (Fig. 4d). A 1 MJ m^{-2} day^{-1} increase in R_s resulted in 0.15 mm day^{-1} and 0.10 mm day^{-1} increase in ETo_{PM} for tropical (Af, Am, As and Aw) and subtropical (Cfa, Cfb, Cwa and Cwb) climates, respectively. As a result of R_s seasonality (Table 2), the sensitivity decreased during winter months in subtropical climates (Cfa, Cfb, Cwa and Cwb) (Fig. 4d). The large sensitivity of ETo_{PM} to R_s has been described in humid climates, even under high temperatures (Irmak et al. 2003). However, the importance of solar radiation in the Penman–Monteith model was observed in cold and wet climates, due to the lower influence of other climatic variables (Hupet and Vanclooster 2001). Comparatively, the sensitivity of ETo_{PM} under humid climates in Changjiang—China, was mainly related to the relative humidity, shortwave radiation and air temperature (Gong et al. 2006). In combination with our results, these findings suggest that the influence of R_s in ETo_{PM} in subtropical climate was subjected to RH and air temperature, which could decrease the VPD and its effect on ETo_{PM}.

The wind speed had a positive effect on ETo_{PM}, showing the second largest importance for all climates (Fig. 3). Increasing U_2 lowers aerodynamic resistance, which increases the ETo_{PM} (Irmak et al. 2006). We observed a diverse effect on ETo_{PM} in different climates. The largest and lowest sensitivity were observed for semiarid (Bsh) and tropical (Af, Am, As and Aw) climates, respectively. A 1 m s^{-1} increase in wind speed resulted in 0.77 mm day^{-1} increase in ETo_{PM} at semiarid conditions. Under wet conditions (Af, Am, As, Aw, Cfa and Cfb), the increase in ETo_{PM} reached

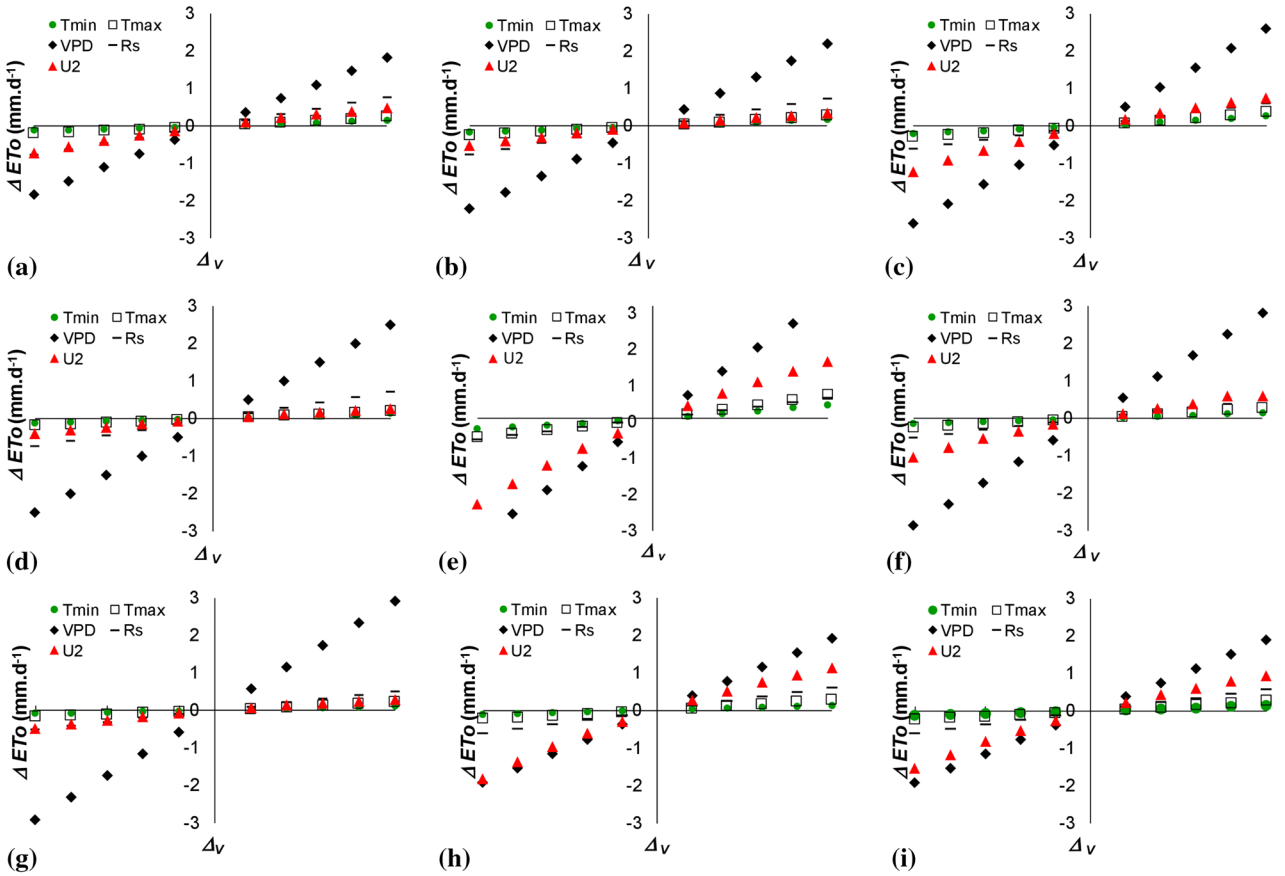

Fig. 3 Annual average variation of ETo_{PM} (mm day^{-1}) as a function of relative changes of climatic variables during the study period for the climate types: Af (**a**), Am (**b**), As (**c**), Aw (**d**), Bsh (**e**), Cfa (**f**), Cfb (**g**), Cwa (**h**) and Cwb (**i**)

only 0.38 mm day^{-1} (Fig. 4e). Under conditions of low relative humidity, the wind replaces the saturated air more efficiently, favoring the maintenance of higher vapor pressure deficits and promoting larger ETo_{PM} (Allen et al. 1998; EMBRAPA—Brazilian Agricultural Research Corporation 2015). Increasing U_2 lower the thickness of the air boundary layer located at the leaf surface, which is described as a mechanism of resistance to the diffusion of water–vapor from leaves to the atmosphere (Nobel 1991). Under semiarid conditions (Bsh), the largest sensitivity was observed during spring and summer months, due to low RH and high air temperature, which favored larger VPD's, improving the effect of U_2 on ETo_{PM}. The strong effect of U_2 over ETo has been also associated to the surface vegetation cover characteristics of the semiarid areas (Haghighi et al. 2017). Those areas are usually covered by short-stature and/or low density tall-stature vegetation, implying in strong near-surface turbulence and negligible radiation effect, mainly at high wind velocity, increasing the evapotranspiration fluxes in soil drying conditions. However, we also observed decrease of evapotranspiration rate in some periods of high solar radiation (data not shown) in the in semiarid climate (Bsh). Under these conditions, leaf surface is usually warmer than surrounding air and the increasing wind speed would might be related to the decrease of evapotranspiration, through enhance of CO_2 uptake and decrease of transpiration flux due to the more efficient convective cooling (Schymanski and Or 2016). In humid subtropical climates with dry winters (Cwa and Cwb), the largest sensitivity was observed during winter months, due to decreased sensitivity to R_s during this period (Fig. 4e).

The highest sensitivity coefficients of air temperature were observed for tropical climates (Af, Am, As and Aw) during spring and summer seasons. In the semiarid climate (Bsh), the sensitivity to air temperature was constant over the year. The variability of sensitivity to air temperature can be explained by its use to the estimation of vapor pressure deficit term, net radiation and longwave radiation balance (Monteith and Unsworth 1990). Compared to other climate variables, the sensitivity coefficients of air temperature were lower and close to zero.

In the subtropical climates (Cfa, Cfb, Cwa and Cwb), the VPD and U_2 coefficients increased during winter, whereas R_s decreased. Similar results were obtained in colder regions (Saxton 1975; Hupet and Vanclooster 2001). Decreasing R_s

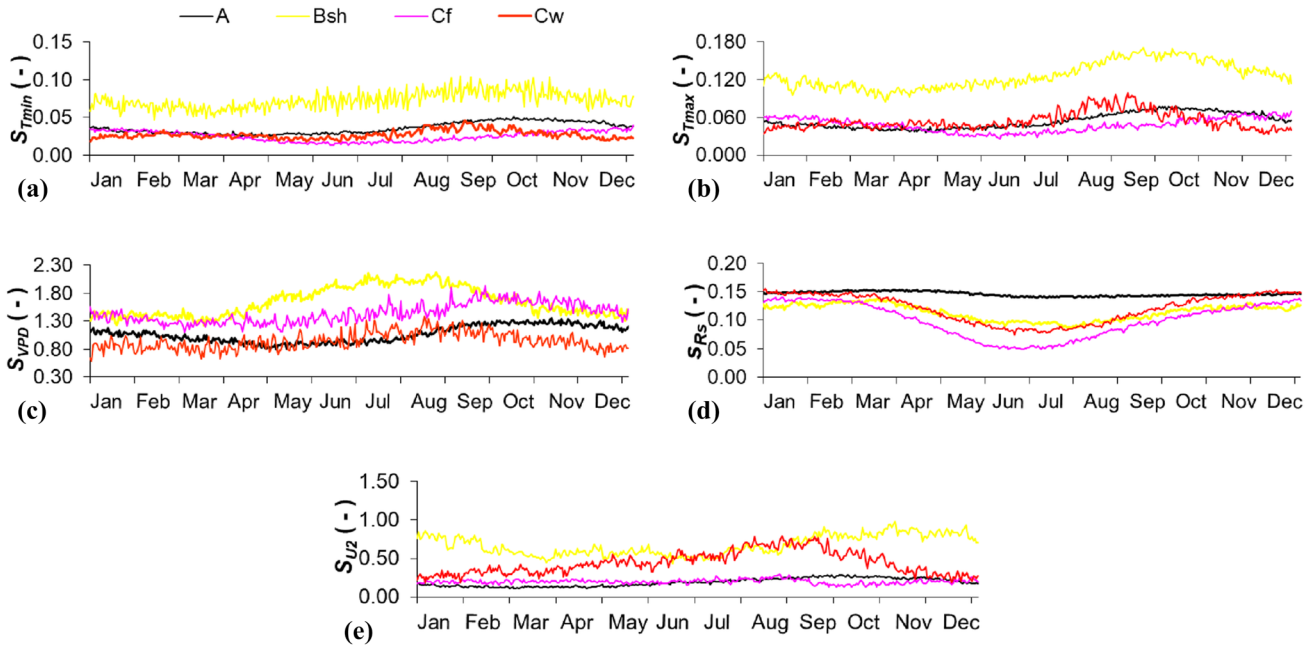

Fig. 4 Monthly average sensitivity coefficients of ETo_{PM} as a response to relative changes of minimum (**a**) and maximum air temperature (**b**), vapor pressure deficit (**c**), solar radiation (**d**) and wind speed (**e**) during the study period for each climate group A (Af, Am, As and Aw), Bsh, Cf (Cfa and Cfb) and Cw (Cwa and Cwb), grouped by its similarity of sensitivity coefficients

sensitivity raises the U_2 sensitivity during winter, due to the importance of aerodynamic component rather than the radiation in the Penman–Monteith model (Saxton 1975; Irmak et al. 2006). As observed in other regions (Rana and Katerji 1998), the exception occurred under semiarid conditions (Bsh), which showed an increase sensitivity to VPD during winter, while decreasing sensitivity to R_s and U_2 (Fig. 4c – 4e). This result suggests the larger effect of VPD on ETo_{PM} under dry conditions.

In the tropical climates (Af, Am, As and Aw), the R_s and U_2 sensitivity coefficients were almost constant throughout the year (Fig. 4d, e). Similar results were obtained under warm and wet conditions (Irmak et al. 2006). This trend was mainly observed in tropical climate with dry summers (As), which showed constant values and small magnitude of sensitivity coefficients for U_2. The strongest and positive correlation between R_s and evapotranspiration has been observed under warm and wet conditions (Wright and Jensen 1972), where the sensitivity of ETo_{PM} to R_s for tropical climates is strongly dependent of its variability throughout the year.

4 Conclusions

The sensitivity of modeled evapotranspiration (ETo_{PM}) to climatic variables was analyzed in tropical, semi-arid, and subtropical climate types throughout Brazil. Five climatic variables were used in the analysis, which revealed a wide range of ETo_{PM} sensitivities across seasons and climatic zones. In order of importance, ETo_{PM} was most sensitive to annual variation in vapor pressure deficit (VPD), wind speed (U_2) and solar radiation (R_s) in all climate types. Our analysis also showed that estimates of VPD by use of reliable measurements of relative humidity (RH) and temperature (T), are essential to accurately predict ETo_{PM} across climatic zones. Due to the lack of direct meteorological measurements in many tropical and subtropical regions, we recommend the adjustment of existing models of climate-driven hydrological fluxes to the most sensitive variables for each climate zone, i.e., VPD, to improve the precision of reference ET estimates and limit the number of input variables in the models. These improved estimates will be useful to better constrain uncertainties in hydrological and climatic predictions in Brazil and elsewhere.

Acknowledgements Coordination for the Improvement of Higher Education Personnel (CAPES/PDSE, Brazil).

References

Allen RG (2008) Quality assessment of weather data and micrometeorological flux impacts on evapotranspiration calculations. J Agric Meteorol 64:191–204

Allen RG, Pereira LS, Raes D, Smith M (1998) Crop evapotranspiration: guidelines for computing crop water requirements, 1st edn. Food and Agriculture Organization of the United Nations, Rome

Allen RG, Walter IA, Elliott R, Mecham B, Jensen ME, Itenfisu D, Howell TA, Snyder R, Brown P, Echings S, Spofford T, Hattendorf M, Cuenca RH, Wright L, Martin D. Issues (2000) Requirements and challenges in selecting and specifying a standardized et equation. pp 201–208. In: Evans RG, Benham BL, Trooien TP (eds) Proceedings of the National Irrigation Symposium, 14–16 Nov 2000, Phoenix, AZ, American Society of Agricultural and Biological Engineers, St. Joseph, MI

Allen RG, Walter IA, Elliott RL, Howell TA, Itenfisu D, Jensen ME, Snyder RL (2005) The ASCE standardized reference evapotranspiration equation. American Society of Civil Engineers, Reston

Álvares CA, Stape JL, Sentelhas PJ, Gonçalves JLM, Sparovek G (2013) Koppen's climate classification map for Brazil. Meteorol Z 22:711–728

Berengena J, Gavilan P. Reference (2005) ET estimation in a highly advective semiarid environment. J Irrig Drain Eng ASCE 131:147–163

Blaney HF, Criddle WD (1950) Determining water requirements in irrigated area from climatological irrigation data. US Department of Agriculture: Soil Conservation Service, Somerset

Butt N, New M, Lizcano G, Malhi Y (2009) Spatial patterns and recent trends in cloud fraction and cloud-related diffuse radiation in Amazonia. J Geophys Res 114:D21104

Carvalho LGC, Rios GFA, Miranda WL, Castro Neto P (2011) Reference evapotranspiration: current analysis of different estimating methods. Pesquisa Agropecuária Tropical 41:456–465

Carvalho LG, Evangelista AWP, Oliveira KMG, Silva BM, Alves MC, Sá Júnior A, Miranda WL (2013) FAO Penman–Monteith equation for reference evapotranspiration from missing data. Idesia 31:39–47

Chen B, Chen JM, Ju W (2007) Remote sensing-based ecosystem–atmosphere simulation scheme (EASS)-model formulation and test with multiple-year data. Ecol Model 209:277–300

Clark DAS, Piper C, Keeling CD, Clark DB (2003) Tropical rain forest tree growth and atmospheric carbon dynamics linked to interannual temperature variation during 1984–2000. Proc Natl Acad Sci 100:5852–5857

EMBRAPA—Brazilian Agricultural Research Corporation (2015) Embrapa Satellite Monitoring. https://www.embrapa.br/en/monitoramento-por-satelite. Accessed 28 July 2016

ESRI ArcGIS Desktop Release 10 (2011) Environmental Systems Research. https://www.esri.com/enus/arcgis/about-arcgis/overview. Accessed 25 July 2016

Estévez J, Gavilán P, Berengena J (2009) Sensitivity analysis of a Penman–Monteith type equation to estimate reference evapotranspiration in southern Spain. Hydrology Processes 23:3342–3353

Fearnside PM (2004) Are climate change impacts already affecting tropical forest biomass? Glob Environ Change 14:299–302

Fisch G, Marengo JM, Nobre CA (1998) The climate of Amazonia: a review. Acta Amazonica 28:101–126

Gatti LV, Gloor M, Miller JB, Doughty CE, Malhi Y, Domingues LG, Basso LS, Martinewski A, Correia CSC, Borges VF, Freitas S, Braz R, Anderson LO, Rocha H, Grace J, Phillips OL, Lloyd J (2014) Drought sensitivity of Amazonian carbon balance revealed by atmospheric measurements. Nature 506:76–80

Gong L, Xu C, Chen D, Halldin S, Chen YD (2006) Sensitivity of the Penman–Monteith reference evapotranspiration to key climatic variables in the Changjiang (Yangtze River) basin. J Hydrol 329:620–629

Goyal RK (2004) Sensitivity of evapotranspiration to global warming: a case study of arid zone of Rajhastan (India). Agric Water Manag 69:1–11

Haghighi E, Kirchner JW (2017) Near-surface turbulence as a missing link in modeling evapotranspiration-soil moisture relationships. Water Resour Res 53:5320–5344

Hijmans RJ, Cameron SE, Parra JL, Jones PG, Jarvis A (2005) Very high resolution interpolated climate surfaces for global land areas. Int J Climatol 25:1965–1978

Hupet F, Vanclooster M (2001) Effect of the sampling frequency of meteorological variables on the estimation of reference evapotranspiration. J Hidrol 243:192–204

INMET—Brazilian National Institute of Meteorology (2014) Meteorological Database for Education and Research (BDMEP). http://www.inmet.gov.br/portal/index.php?r=bdmep/bdmep. Accessed 15 June 2014

Irmak S, Irmak A, Allen RG, Jones JW (2003) Solar and net radiation-based equations to estimate reference evapotranspiration in humid climates. J Irrig Drain Eng ASCE 129:336–347

Irmak S, Payero JO, Martin DL, Irmak A, Howell TA (2006) Sensitivity analyses and sensitivity coefficients of standardized daily ASCE-Penman–Monteith equation. J Irrig Drain Eng 132:564–578

Itenfisu D, Elliott RL, Allen RG, Walter IA (2003) Comparison of reference evapotranspiration calculations as part of ASCE standardization effort. J Irrig Drain Eng 129:440–448

Jasechko S, Sharp ZD, Gibson JJ, Birks SJ, Yi Y, Fawcett PJ (2013) Terrestrial water fluxes dominated by transpiration. Nature 496:347–350

Jerszurki D, Couvreur V, Maxwell T, Silva LCR, Matsumoto N, Shackel K, Souza JLM, Hopmans J (2017) Impact of root growth and hydraulic conductance on canopy carbon-water relations of young walnut trees (*Juglans regia* L.) under drought. Sci Hortic 226:342–352

Lemos Filho LCA, Mello CR, Faria MA, Carvalho LG (2010) Spatial-temporal analysis of water requirements of coffee crop in Minas Gerais State, Brazil. Revista Brasileira de Engenharia Agrícola e Ambiental 14:165–172

Liqiao L, Lijuan L, Li Z, Jiuyi L, Dejuan J, Mingxing X, Wenxian S (2008) Sensitivity of the reference crop evapotranspiration in growing season in the West Songnen Plain. Trans Chin Soc Agric Eng 18:340–347

MAPA—Brazilian Ministry of Agriculture, Livestock and Food Supply (2016) Food exportation. http://www.agricultura.gov.br/vegetal/exportacao. Accessed 29 Dec 2016

Maxwell T, Silva LCR, Horwath W (2014) Using multi-element isotopic analysis to decipher drought impacts and adaptive management in ancient agricultural systems. Proc Natl Acad Sci 45:4807–4808

Maxwell T, Silva LCR, Horwath WR (2018) Integrating effects of species composition and soil properties to predict shifts in montane forest carbon–water relations. Proc Natl Acad Sci 115:4219–4226

Monteith JL (1965) Evaporation and environment. In: 19th symposia of the Society for Experimental Biology. University Press, Cambridge, pp 205–234

Monteith JL. Evaporation and environment (1964) In the state and movement of water in living organisms. Symp Soc Exp Biol 19:205–234

Monteith JL, Unsworth MH (1990) Principles of environmental physics, 2nd edn. Edward Arnold, New York

Murray FW (1967) On the computation of saturation vapor pressure. J Appl Meteorol 6:203–204

Nobel PS (1991) Physicochemical and environmental plant phisiology, 1st edn. Academic Press, San Diego

Pereira AR, Sentelhas PC, Folegatti MV, Villa Nova NA, Maggiotto SR, Pereira FAC (2002) Substantiation of the daily FAO-56 reference evapotranspiration with data from automatic and conventional weather stations. Revista Brasileira de Agrometeorologia 10:251–257

Pereira LS, Allen LG, Smith M, Raes D (2015) Crop evapotranspiration estimation with FAO56: past and future. Agric Water Manag 147:4–20

Rana G, Katerji N (1998) A measurement based sensitivity analysis of the Penman–Monteith actual evapotranspiration model for crops of different height and in contrasting water status. Theor Appl Climatol 60:141–149

Saxton KE (1975) Sensitivity analysis of the combination evapotranspiration equation. Agric Meteorol 15:343–353

Schymanski SJ, Or D (2016) Wind increases leaf water use efficiency. Plant Cell Environ 39:1448–1459

Shaw EM (1993) Hydrology in practice, 3rd edn. Chapman and Hall, London

Silva LCR (2015) From air to land: understanding water resources through plant-based multidisciplinary research. Trends Plant Sci 20:399–401

Silva LCR, Anand M (2013) Historical links and new frontiers in the study of forest–atmosphere interactions. Community Ecol 14:208–218

Silva AO, Moura GBA, Silva EFF, Lopes PMO, Silva APN (2011) Spatio-temporal analysis of reference evapotranspiration under different regimes of precipitation in Pernambuco. Revista Caatinga 24:135–142

Silva LCR, Pedroso G, Doane TA, Mukome FND, Horwath WD (2015) Beyond the cellulose: oxygen isotope composition of plant lipids as a proxy for terrestrial water balance. Geochem Perspect Lett 1:33–42

Smajstrla AG, Zazueta FS, Schmidt GM (1987) Sensitivity of potential evapotranspiration to four climatic variables in Florida. Soil Crop Sci Soc Fla 46:21–26

Souza JLM, Fezer KF, Gurski BC, Jerszurki D, Pachechenik PE (2016) Soil water balance in different densitites of *Pinus taeda* in Southern Brazil. Acta Sci 38:265–271

Sulman BN, Roman DT, Yi K, Wang L, Phillips RP, Novick KA (2016) High atmospheric demand for water can limit forest carbon uptake and transpiration as severely as dry soil. Geophys Res Lett 43:9686–9695

Walter IA, Allen RG, Elliott R, Jensen ME, Itenfisu D, Mecham B et al (2000) ASCE's standardized reference evapotranspiration equation. In: National irrigation symposium, 4. 2000 Phoenix. Proceedings, vol 1. American Society of Agricultural Engineers, Phoenix, pp 209–215

Wang K, Dickinson RE (2012) A review of global terrestrial evapotranspiration: observation, modeling, climatology and climatic variability. Rev Geophys 50:1–54

Wright JL, Jensen ME (1972) Peak water requirements of crops in southern Idaho. J Irrig Drain Eng 98:193–201

Xu CY, Singh VP (2005) Evaluation of three complementary relationship evapotranspiration models by water balance approach to estimate actual regional evapotranspiration in different climatic regions. J Hidrol 308:105–121

Yan H, Wang SQ, Billesbach D, Oechel W, Zhang JH, Meyers T et al (2012) Global estimation of evapotranspiration using a leaf area index-based surface energy and water balance model. Remote Sens Environ 124:581–595